Foam stability in gas injection foaming process

Xing Nan Liu · Yan Xiang Li · Xiang Chen ·
Yuan Liu · Xue Liu Fan

Abstract Particle coverage ratio on bubble interface was investigated by metallographic analysis when the foam is critically stable in the gas injection foaming process. It is found that the critical coverage ratio was almost the same under different conditions, such as different particle amount, particle size, or particle wettability. The particle coverage ratio is proposed as the criterion to judge the foam stability, and a criterion equation was deduced. Adsorption coefficient of particles, effective coverage ratio of a particle and critical coverage ratio on the bubble interface are stability influencing parameters of the criterion equation. Their determination methods were presented and examined by air injection foaming of A356/Al$_2$O$_3$ melt. The adsorption coefficient calculated by measuring cross-section of foam cell wall gave values agreeing with the experimental results. The effective coverage ratio, which is about 0.9 in this article, can be calculated by combining measurements on surface and on the cross-section of the foam cell wall. The critical coverage ratio, that is about 14% in this article, can be determined by measuring the cross-section as well as the surface of the foam cell wall.

X. N. Liu · Y. X. Li (✉) · X. Chen · Y. Liu · X. L. Fan
Department of Mechanical Engineering, Tsinghua University,
Beijing 100084, People's Republic of China
e-mail: yanxiang@tsinghua.edu.cn

Y. X. Li · X. Chen · Y. Liu
Key Laboratory for Advanced Materials Processing Technology,
Ministry of Education, Beijing 100084,
People's Republic of China

List of symbols

A_b	Equator area of a bubble in Eq. 1 (cm^2)
E_k	Adsorption coefficient of particles in Eq. 1
h	Nozzle immersion depth in Eq. 1 (cm)
N_P^*	Critical number of particles required to stabilize the bubble in Eq. 1
V_P	Volume of a single particle in Eq. 1 (cm^3)
vol.%	Particle volume percentage in Eq. 1 (%)
β^*	Critical foam stability parameter in Eq. 1 (cm)
A	Coverage area of particles on the bubble interface (mm^2)
D	Diameter of a bubble, or pore size in the foam (mm)
d	Diameter of particles (mm)
d'	Two-dimensional diameter of particles measured by metallographic analysis (mm)
d_a	Two-dimensional diameter of particles on the bubble interface (measured on the surface of the foam cell wall by metallographic analysis) (mm)
d_l	Two-dimensional diameter of particles on the bubble interface (measured on the cross-section of the foam cell wall by metallographic analysis) (mm)
$d_1,\dots,d_n$	Diameter of different sections of particle when measuring two-dimensional diameter of the particle by metallographic analysis (mm)
E	Effective coverage ratio of a particle, "effective coverage ratio" for short
F_V	Volume percentage of particles in the melt (%)
F_{Vf}	Volume percentage of particles in the foam (%)
F_{Vf}'	F_{Vf} calculated by Eq. 13 (%)
F_{Vf}''	F_{Vf} calculated by Eq. 21 (%)
F_{Vf1}	Volume percentage of particles attached on the gas/solid interface (%)

F_{Vf2}	Volume percentage of particles embedded inside the foam cell wall (%)
F_{WCa}	Weight percentage of calcium (%)
h	Nozzle immersion depth (mm)
h_c	Nozzle immersion depth at which the foam is critically stable (mm)
k	Ratio of particles partial volume protruding into the gas to V_P
n	Number of particles adsorbed by one bubble
R	Correction coefficient in Eq. 21
t	Thickness of the foam cell wall (mm)
V_P	Total volume of particles adsorbed by one bubble (mm^3)
W	Adsorption coefficient of particles
W_a	W determined as Eq. 7
W_l	W determined as Eq. 9
W_V	W determined according to Eq. 13
β	Critical particle coverage ratio on the bubble interface, "critical coverage ratio" for short
β_a	β determined by directly measuring on the surface of critically stable foam cell wall
β_l	β determined according to Eq. 20
θ	Wetting angle of particles (°)
ρ_a	Number of particles per unit area on the bubble interface (measured on the surface of the foam cell wall), "particle area density" for short (mm^{-2})
ρ_l	Linear density of particles on the bubble interface (measured on the cross-section of the foam cell wall), "particle linear density" for short (mm^{-1})

Introduction

Aluminum foams appeal people's more and more attentions. They can be used alone, or made into hybrid materials to get special properties [1–3]. Among the methods could be used to fabricate aluminum foams [4–6], gas injection foaming is one of the most promising processes. In this process, gas bubbles are directly injected into the molten aluminum to make foams on the melt surface [7]. This method can produce foams both in continuous way and in batch type [7, 8]. Comparing with the Alporas melt foaming process and powder compact melting foaming method, it has the advantages of low cost, and is suitable for volume production and near net shape forming of complex parts [4–6]. Besides, it is easier to produce foams with big pore size and high porosity [7, 8].

In other processes for producing aluminum foams, adding particles is usually a better selection to enhance foam stability [9]. However, it is the necessary condition

for the gas injection foaming process [10, 11]. Up to now very few understanding about stabilization mechanism of metal foam in this process is put forward [12]. Actually, the following conditions have been considered: the particles reduce free energy of the foam by covering the bubble interface [13]; the particles obstruct drainage inside the foam cell wall [14]; the particles enhance the foam cell wall's capacity of resisting disturbance [15]. For all these considerations, the necessary condition is that there must have enough particles in the foam. The relationship between minimum amount of particle in the melt and the nozzle immersion depth has been reported [8]. Ip et al. [16] even proposed a concept of "critical foam stability parameter" β^*, which is based on a critical number of particles required to stabilize the bubble N_P^*, which is shown in Eq. 1:

$$N_p^* \cdot \frac{V_P}{A_b E_k} = \frac{vol.\%}{100}h = \beta^* \tag{1}$$

where V_P denotes the volume of a single particle, A_b the equator area of a bubble, E_k the adsorption coefficient of particles, vol.% the particle volume percentage, and h the nozzle immersion depth. Although Eq. 1 does not reveal the stabilization mechanism, it is helpful to understand how the foam can be stabilized. Unfortunately, Eq. 1 does not reflect the wettability of particles, which affects the foam stability strongly in the gas injection foaming process [17]. Therefore, the critical foam stability parameter β^* needs to be further studied.

Metallic foam is usually simulated with the foam in water solution to research the stabilization mechanism [17, 18]. Some researchers found that wettable particles can stabilize the foam, and the wetting angle near 90° is in favor of the foam stability [17]. Sun et al. [18] found that the particles whose wetting angle is larger than 90° could stabilize the foam also, if the angle was not too large, i.e., 100°. Besides, Kaptay [19] developed a theory to predict the optimum wetting angle of particles when stabilizing emulsions and foams, and 70°–86° was deduced for actual condition in particle stabilized aluminum foams, which was proved to be a general guide to select foaming system by Klinter et al. [20]. In a word, almost all researchers consider that there exist an optimum wetting angle for particles to stabilize the foams, and most researches consider the optimum angle as about 90°.

Either the number of particles adsorbed by the bubbles is enough, or particle wetting angle is close to 90°, the coverage area on the bubble interface by particles will be large. Therefore, the authors propose such a viewpoint that, the larger the coverage ratio on the bubble interface, the more stable the foam will be. As the foam stability is actually a relative concept, the foam will be stabilized when coverage ratio on the bubble interface is lager than a critical value under certain condition.

Based on these analyses, a criterion called "critical particle coverage ratio on the bubble interface" is proposed firstly in this article, and then the determination of parameters in the criterion equation is discussed, and finally A356/Al$_2$O$_3$ air foaming experiments were done to prove the criterion and examine the determining methods.

The foam stabilization criterion

Figure 1 is the schematic sketch of the bubble rising process. In Fig. 1, D is the bubble diameter, h the nozzle immersion depth, F_V the volume percentage of particles in the melt, d the particle diameter, and W the adsorption coefficient of particles.

During the bubble rising, the number of particles adsorbed by the bubble, n, can be calculated by Eq. 2:

$$n = \frac{\frac{\pi}{4}D^2 h F_V W}{\pi d^3 / 6} = \frac{3D^2 h F_V W}{2d^3}. \tag{2}$$

Then the coverage area of particles on the bubble interface, A, is:

$$A = n \cdot \frac{\pi d^2}{4} \cdot E \tag{3}$$

where E, effective coverage ratio of a particle, is the ratio of the coverage area (dashed circle) to the equator area of the particle in Fig. 2, where θ is the wetting angle of particles.

Based on the criterion mentioned above, the foam will be stable when the ratio of the coverage area to the total interface area is larger than a critical coverage ratio β. Thus, the stabilization criterion can be expressed as:

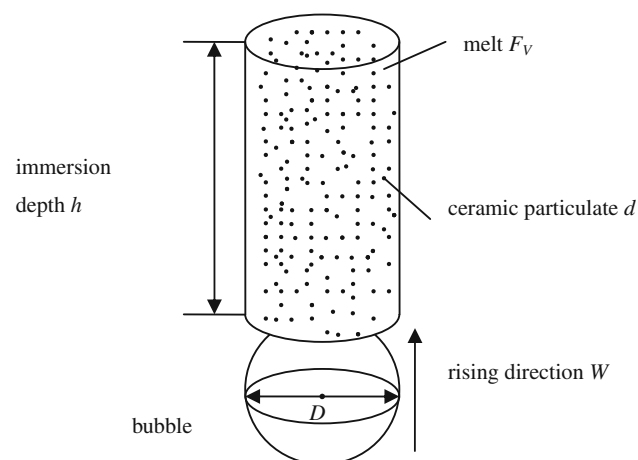$$\frac{A}{\pi D^2} = \frac{3hF_V W E}{8d} \geq \beta \tag{4}$$

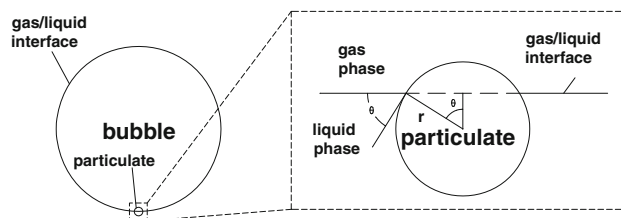Fig. 1 Schematic sketch of bubble rising process

Fig. 2 Schematic sketch of particle adsorbed on the bubble interface

or

$$h \cdot F_V \geq \frac{8d\beta}{3WE}. \tag{5}$$

Equation 5 is the expression of the critical coverage ratio criterion of foam stabilization in the gas injection process.

Determination method for parameters in stabilization criterion

It is necessary to determine the six parameters in Eq. 5 for quantitative application. Among these parameters, W, E, and β are stability influencing parameters. They are different from process parameters such as h, F_V, and d. Though the stability influencing parameters are relatively fixed in a given foaming processing, they are difficult to obtain. Some methods are proposed as follows.

Adsorption coefficient W

The adsorption coefficient W is a dependant parameter influenced by other parameters, such as wettability of particles, diameter of bubbles, diameter of particles etc. It usually needs to be determined by experiments.

W could be determined by measuring particle area density on the bubble interface, ρ_a, which is the number of particles per unit area on the bubble interface. According to Eq. 2, ρ_a can be written as Eq. 6:

$$\rho_a = \frac{n}{\pi D^2} = \frac{3hF_V W}{2\pi d^3}. \tag{6}$$

ρ_a could be measured by metallographic analysis on the surface of the foam cell wall, and then W could be calculated by Eq. 7:

$$W = \frac{2\pi d^3}{3hF_V}\rho_a. \tag{7}$$

Similarly, W could be determined by measuring particle linear density on the bubble interface, ρ_l. In fact, ρ_l and ρ_a have a relationship as that in Eq. 8:

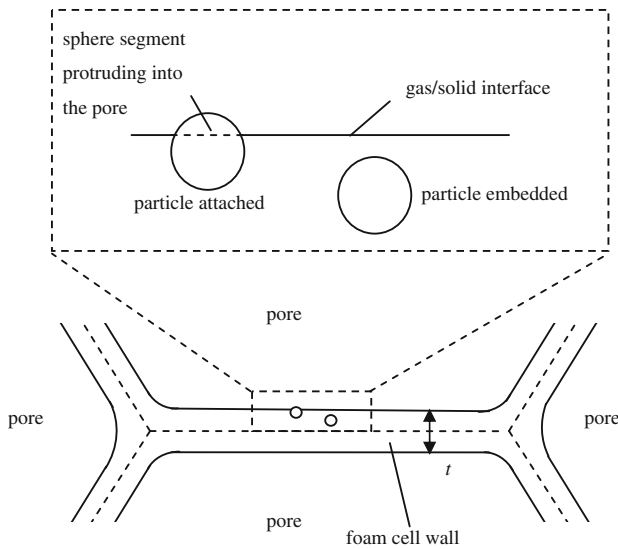$$\rho_a = \frac{\rho_l}{d}. \tag{8}$$

Fig. 3 Schematic sketch of particles in the foam

ρ_l could be measured by metallographic analysis on cross-section of the foam cell wall, and then W could be attained by Eq. 9:

$$W = \frac{2\pi d^2}{3hF_V}\rho_l. \tag{9}$$

In addition, W could be determined by measuring particles amount in the foam. Particles in the foam comprise two parts, like Fig. 3, one attached on the gas/solid interface, which are absorbed by the bubble during rising, and the other embedded inside the foam cell wall.

The volume percentage of particles attached on the gas/solid interface, F_{Vf1}, is given in Eq. 10:

$$F_{Vf1} = \frac{V_p}{\pi D^2 \frac{t}{2} + kV_p} = \frac{F_V hW}{2t + kF_V hW}, \tag{10}$$

where V_P is total volume of particles adsorbed by one bubble, t the thickness of the foam cell wall, and k the ratio of particles partial volume protruding into the gas to V_P (equal to the ratio of the sphere segment volume to the entire sphere volume). According to Fig. 2, k can be expressed as Eq. 11:

$$k = \frac{(1 - \cos\theta)^2 (2 + \cos\theta)}{4}. \tag{11}$$

The volume percentage of particles embedded inside the foam cell wall, F_{Vf2}, is given by Eq. 12:

$$F_{Vf2} = \frac{\left[(\pi D^2 \frac{t}{2} + kV_p) - V_p\right]F_V}{\pi D^2 \frac{t}{2} + kV_p} = F_V - \frac{F_V hW}{2t + kF_V hW}F_V. \tag{12}$$

Here, it needs to suppose that the drainage is little during forming and solidification processes. According to literature [11], this supposition is reasonable when the

particle amount in the foam is large and the oxygen content in the foaming gas is high.

The volume percentage of particles in the foam, F_{Vf}, could be expressed as Eq. 13:

$$F_{Vf} = F_{Vf1} + F_{Vf2} = F_V\left[\frac{(1 - F_V)hW}{2t + kF_V hW} + 1\right]. \tag{13}$$

The values of F_{Vf} and t could be measured on cross-section of cell wall by metallographic analysis, and θ could be calculated also (see "Effective coverage ratio of a particle E" section). Then, W could be determined by Eq. 13.

Effective coverage ratio of a particle E

The effective coverage ratio of a particle E depends on wettability of the particle. According to Fig. 2, E is

$$E = \sin^2\theta. \tag{14}$$

It needs measurement in experiment, as θ changes with experimental conditions [18, 21–24].

Parameters d_a and d_l, which are measured on the surface and on the cross-section of the foam cell wall by metallographic analysis, respectively, can be defined as two-dimensional diameters of a particle on the bubble interface. The real diameter of particles on the bubble interface d can be calculated by d_l with Eq. 15:

$$d = \frac{4}{\pi}d_l. \tag{15}$$

According to Fig. 2, E and θ could be expressed as Eqs. 16 and 17, respectively:

$$\theta = \arcsin\frac{\pi d_a}{4d_l}, \tag{16}$$

$$E = \frac{\pi^2 d_a^2}{16d_l^2}. \tag{17}$$

It is necessary to explain that d and d', which is two-dimensional diameter of particles measured by metallographic analysis, have a relationship of Eq. 18 (see Appendix for details):

$$d = \frac{4}{\pi}d'. \tag{18}$$

Critical coverage ratio on the bubble interface β

The direct method to determine the critical coverage ratio β is to measure area percentage of particles on the bubble interface by observing the surface of the critically stable foam cell wall.

Besides, it also can be obtained by the relationship between β and ρ_a of the critically stable foam cell wall, as in Eq. 19:

$$\beta = \rho_a\frac{\pi}{4}d^2\sin^2\theta. \tag{19}$$

Substituting Eq. 8 in Eq. 19, β can be attained by

$$\beta = \rho_1 \frac{\pi}{4} d \sin^2 \theta. \tag{20}$$

Therefore, β could be determined by measuring ρ_1 of the critically stable foam cell wall.

Experimental

Materials and instruments

The base material used in experiments is A356 aluminum alloy, which was melted in a crucible furnace. Some Al_2O_3 particles, with size of 9, 15, or 23 μm, were added into the A356 melt, and dispersed by mechanical stirring. Then, compressed air was injected into the melt through certain nozzle to make the foam.

Two types of nozzles were used. The first type of nozzle was a long pipe made of a stainless steel with the inside and outside diameter of 1 and 3 mm respectively, as shown in Fig. 4. It was immersed into the melt from top, and the immersion depth could be adjusted by the positioning screw and holder. The foam produced with this nozzle had a pore size of 15–20 mm.

The second type of nozzle was a porous plug with special configuration, which was installed at the bottom of the foaming mold, which is shown in Fig. 5. The foam produced with this nozzle in our experimental conditions had a pore size of 10–15 mm.

Methods and steps

The first part of the experiment

The first part was done to prove the criterion, and the first type of nozzle (Fig. 4) was used. The foam would not be stabilized until the immersion depth of nozzle is larger than some critical value when other parameters are fixed [8]. In this part of experiment, the immersion depth was increased gradually until the foam was stabilized. The critical immersion depth h_c was recorded. The experiment was repeated till two consecutive measurements were consistent. And the critically stable foams were collected. The "stable foam" means the foam would not collapse after gas injection. Foaming time was 30 s and holding time was 90 s. The air flow was 40–67 L/h, and the gas pressure in gas chamber was below 1.1 atm. The foaming temperature was 700 °C.

Particle amount, particle size, and particle wettability are the most important parameters in foaming process. The effects of these parameters on β were investigated to prove the criterion. Six types of melts, which are shown in
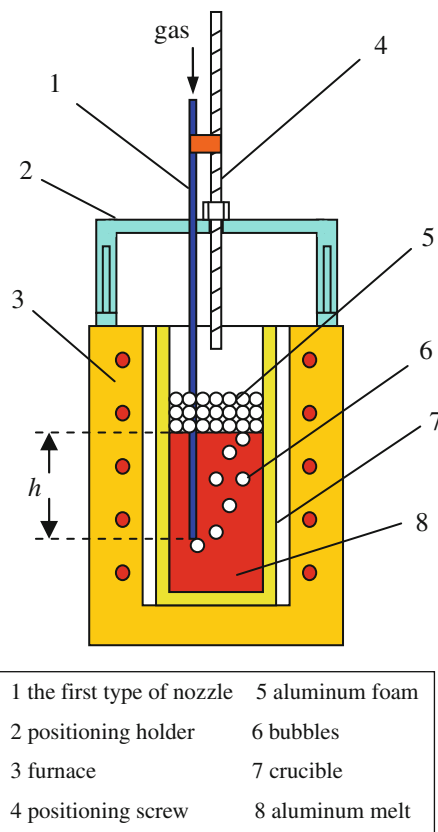

1 the first type of nozzle	5 aluminum foam
2 positioning holder	6 bubbles
3 furnace	7 crucible
4 positioning screw	8 aluminum melt

Fig. 4 Diagram of foaming process using the first type of nozzle

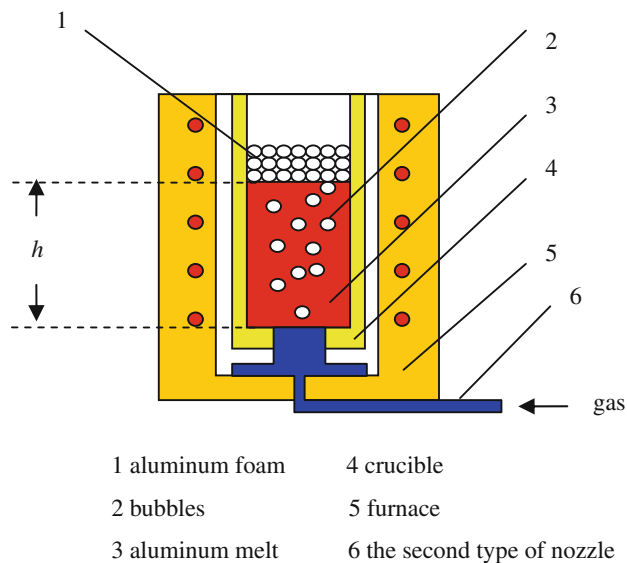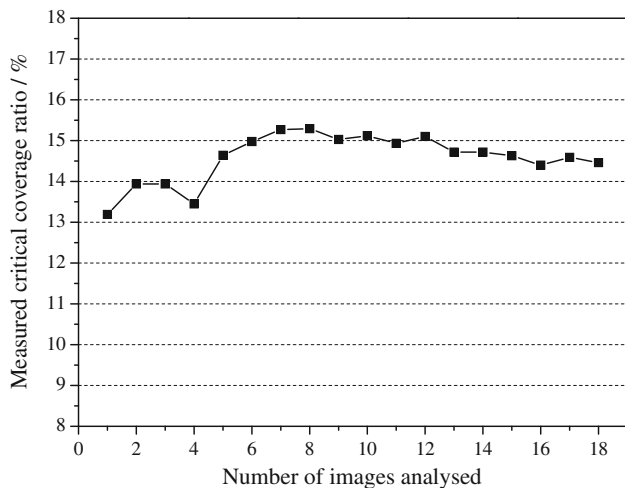| 1 aluminum foam | 4 crucible |
| 2 bubbles | 5 furnace |
| 3 aluminum melt | 6 the second type of nozzle |

Fig. 5 Diagram of foaming process using the second type of nozzle

Table 1, were foamed. For melt 6, the particle wettability was changed by adding calcium. β was measured on the surface of critically stable foam cell wall. For every type of melt, 3–5 pieces of cell walls were polished, photographed, and quantitatively analyzed on a Neophot 32 microscope

Table 1 Six types of melt foamed in the first part of experiment

Melt no.	Particle size $d \times 10^3$ (mm)	Particle amount F_V (%)	Ca amount F_{WCa} (%)
1	9	3	0
2	9	5	0
3	9	8	0
4	15	5	0
5	23	5	0
6	15	5	1

Fig. 6 Relationship of measured critical coverage ratio, β, and number of analyzed images

with image analysis software. According to our test, the measured value of β would be steady (Fig. 6) when the field number (size of 440 μm * 330 μm) observed is larger than 14. Thus a total of 15–18 fields were measured on each specimen in this study.

The second part of the experiment

The second part of experiment was done to examine the determination methods of W, E, and β, with the second type of nozzle (Fig. 5). The very beginning, 10 vol.% 9 μm Al_2O_3 particles were added into certain amount of A356 melt, without calcium. During foaming process, because of the adsorption of particles by bubbles, both particle amount and immersion depth decreased till the foam was critically stable. Gas injection was discontinuous. Prior to each injection, three pieces of melt samples were taken out from different position of the melt, and h was recorded. Foam was collected after each injection. Four foam samples were analyzed, samples I, II, III, and IV. They were foamed in chronological order. Foam sample IV was critically stable, after which foam was not stable any longer.

First, F_V and d in melt sample I were measured. Three melt samples, which were all signed as "sample I," were analyzed on the Neophot 32 microscope with image analysis software. F_V and d would be steady when the field number (size of 888 μm * 666 μm) observed is greater than 12.

Then, both the surface and the cross-section of cell wall of foam sample I were observed. At least three pieces of the foam cell walls were analyzed to observe the surface, and four pieces for the cross-section. The fields were all size of 440 μm * 330 μm. W was calculated according to Eqs. 7, 9, and 13, respectively. The three methods were compared and an applicable method under this experimental condition was found. E was determined with Eq. 17. Except for h, F_V, and d, these calculations need the values of ρ_a, ρ_l, F_{Vf}, t, k, d_a, and d_l. According to our test, ρ_a and d_a need measuring 14 fields at least, ρ_l and d_l 15 fields, t 16 fields, and F_{Vf} 17 fields. k is calculated by Eqs. 11 and 16.

Similarly, foam samples II, III, IV and their corresponding melt samples were all analyzed to determine W, with the applicable method.

At last, the critical coverage ratio β of foam sample IV was determined with direct method and Eq. 20 respectively.

All the arrangements for experiments in the second part are listed in Table 2. The air flow was 16–40 L/h, and the foaming temperature is 700 °C.

Results

The first part of experiment

Effect of particle volume percentage on critical coverage ratio

The foam sample and the metallograph of cell wall surface are shown in Fig. 7. Based on analysis on the metallographs of cell wall surface shown in Fig. 7b, the critical nozzle immersion depth and the critical coverage ratio on the bubble interface in the melt, which contains 3, 5, and 8 vol.% 9 μm Al_2O_3 particles respectively, are shown in Table 3. According to Table 3, the critical coverage ratio β on the bubble interface in the melts containing different amounts of particles is almost a constant. The critical nozzle immersion depth increases with the decreasing of particle volume percentage, and they show roughly a reverse proportional relationship.
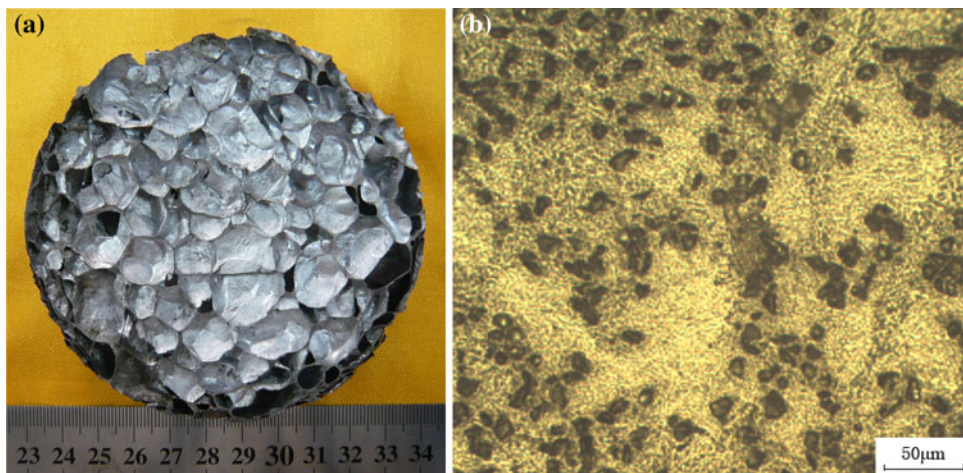
Effect of particle size on critical coverage ratio

Table 4 shows, the critical nozzle immersion depth and the critical coverage ratio on the bubble interface in the melt,

Table 2 Parameters measured in the second part of experiment (dot marked)

Sample no.	Parameter				
	Particle amount in the melt sample F_V	Particle size in the melt sample d	Adsorption coefficient W	Particle effective coverage ratio E	Critical coverage ratio β
I	•	•	•	•	
II	•	•	•		
III	•	•	•		
IV	•	•	•		•

Fig. 7 Photograph of aluminum foam (**a**) and metallograph of foam cell wall surface (**b**)

which contains 5 vol.% Al_2O_3 particles size of 9, 15, and 23 μm, respectively. It can be seen from Table 4 that the critical coverage ratio on the bubble interface in the melts, which contain different sizes of particles is almost a constant. The critical nozzle immersion depth increases as particle size increases.

Table 3 Volume percentage (F_V) of particles (9 μm), corresponding critical nozzle immersion depth (h_c), and the critical coverage ratio (β)

Melt no.	F_V (%)	h_c (mm)	β (%)
1	3	110	14.6
2	5	60	13.7
3	8	45	14.5

Table 4 Diameter (d) of particles (5 vol.%), corresponding critical nozzle immersion depth (h_c), and the critical coverage ratio (β)

Melt no.	$d \times 10^3$ (mm)	h_c (mm)	β (%)
2	9	60	13.7
4	15	70	14.0
5	23	120	13.3

Effect of particle wettability on critical coverage ratio

The critical nozzle immersion depth and the critical coverage ratio on the bubble interface in the melt, which contains 5 vol.% 15 μm Al_2O_3 particles and with or without 1.0 wt% Ca are listed in Table 5. Based on Table 5, the critical coverage ratio on the bubble interface in the melt with or without Ca is almost the same. The critical nozzle immersion depth increases a little with Ca addition.

The second part of experiment

Analysis of melt sample I

Metallograph of melt sample I is shown in Fig. 8. The black granular or aggregations are Al_2O_3 particles. It can be seen

Table 5 Weight percentage of Ca (F_W) in the melt, which contains 5 vol.% 15 μm Al_2O_3, and corresponding critical nozzle immersion depth (h_c), and the critical coverage ratio (β)

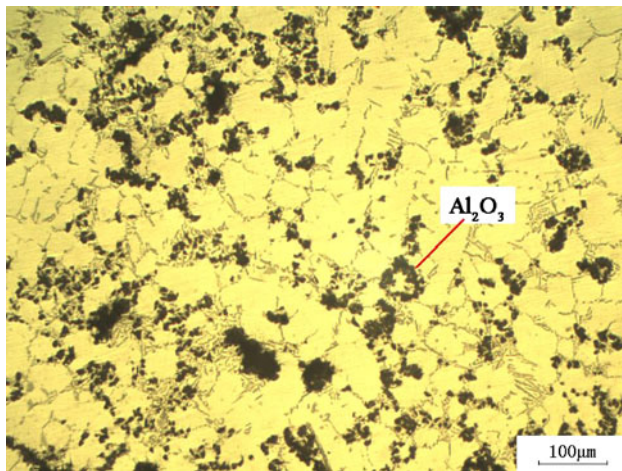| Melt no.	F_{WCa} (%)	h_c (mm)	β (%)
4	0.0	70	14.0
6	1.0	90	13.4

Fig. 8 Metallograph of melt sample I (from which foam sample I was produced)
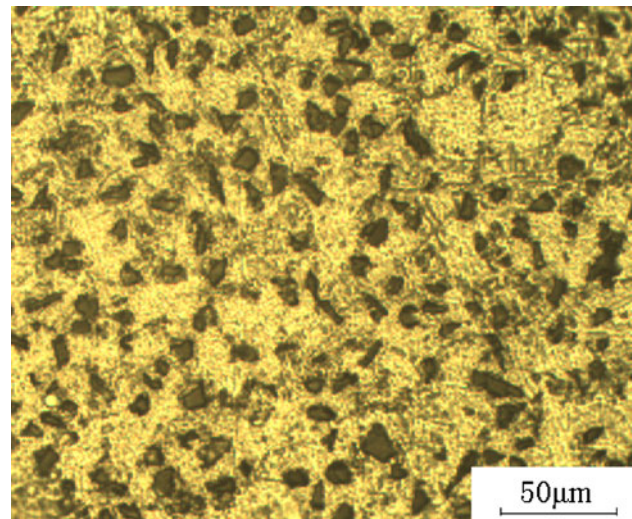

Fig. 9 Metallograph of surface of cell wall of foam sample I

Table 6 Particle volume percentage (F_V), real average diameter (d) of particles in the melt sample I, and nozzle immersion depth (h)

Specimen	F_V (%)	$d \times 10^3$ (mm)	h (mm)
Melt sample I	13.27	17.37	125

in Fig. 8, some particles agglomerated owing to difficulty dispersion of particles. The measurement results of sample I are listed in Table 6 by analyzing 15 images.

Adsorption coefficient W of foam sample I

There are three methods to calculate the adsorption coefficient W as Eqs. 7, 9, 11, and 13.

Firstly, W is determined as Eq. 7 by measuring ρ_a, which is denoted as W_a. Figure 9 is metallograph of the surface of the cell wall of foam sample I. Fifteen images are analyzed, and ρ_a and W_a are listed in Table 7.

Secondly, W is determined as Eq. 9 by measuring ρ_l, which is denoted as W_l. Figure 10a is metallograph of the cross-section of the cell wall of foam sample I. Markings in Fig. 10a are used to measure length of the interface. Figure 10b shows particles on the bubble interface. Linear density ρ_l is measured by analyzing images like Fig. 10b with software. Twenty-four images are analyzed, and ρ_l and W_l are listed in Table 7.

At last, W is determined through Eq. 13 by measuring F_{Vf} of the cell wall of foam sample I, which is denoted as W_V. F_{Vf} is also measured on the cross-section. Particles in the cross-section are highlighted like Fig. 11. Twenty-four images are analyzed, and F_{Vf} is listed in Table 7.

According to Eqs. 11 and 13, the determination of W_V needs thickness of cell wall t and wetting angle θ additionally. The thickness t is measured on images like Fig. 12. Twenty-four images are analyzed, and measured value is listed in Table 7. The wetting angle θ is gotten from Table 8, and the measurement will be introduced below.

Measured results of the three methods determining W above mentioned are listed in Table 7. Some parameters used in calculation are from Table 6 (F_V, d, and h) and Table 8 (θ).

Effective coverage ratio E of foam sample I

d_a and d_l denote average diameter of particles in Figs. 9 and 10b, respectively. The real diameter of particles on the bubble interface d, E, and θ is calculated by Eqs. 15, 16, and 17, respectively. The results are listed in Table 8.

Critical coverage ratio β of foam sample IV

Firstly, β is determined by directly measurement like the first part of experiment on the surface of critically stable foam sample IV, which is denoted as β_a. Sixteen images are analyzed, and the result is listed in Table 9.

And then, β is determined according to Eq. 20, which is denoted as β_l. Eighteen images are analyzed to determine ρ_l of foam sample IV and 17 images are analyzed to determine d in the melt sample IV. θ used in calculation is gotten from Table 8.

The results of the direct and indirect determination methods are listed in Table 9.

Table 7 Adsorption coefficient of foam sample I

Specimen	ρ_a (mm^2)	W_a	ρ_l (mm^{-1})	W_l	F_{Vf} (%)	$t \times 10^3$ (mm)	W_V
Foam sample I	2680.8	0.0018	28.95	0.0011	20.15	126.74	0.0012

Fig. 10 Cross-section of cell wall of foam sample I: **a** photo and markings of length of interface; **b** highlight of particles on the bubble interface
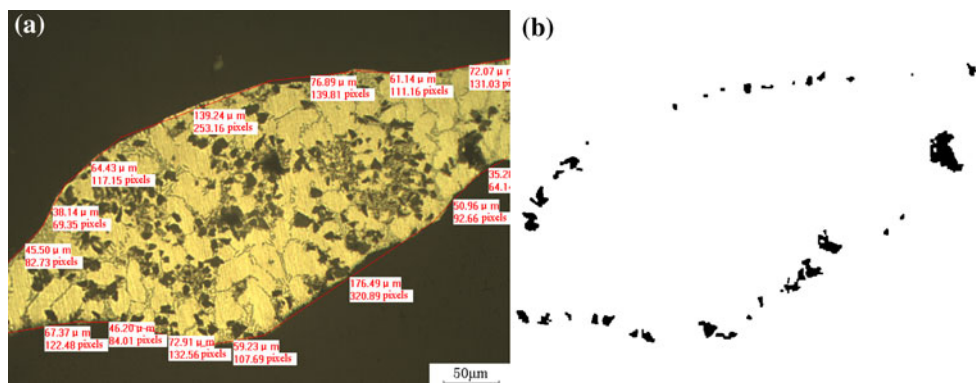

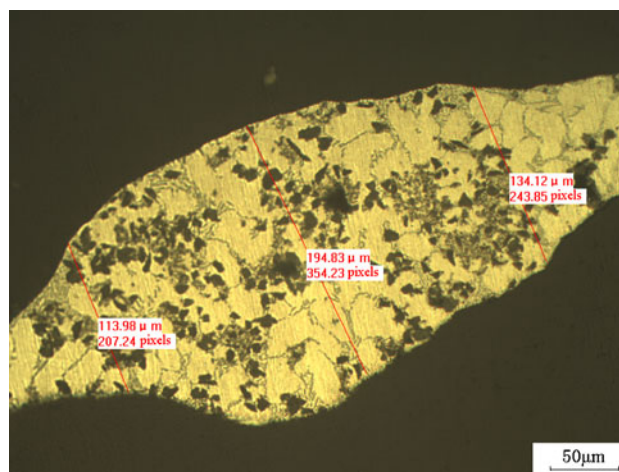**Fig. 11** Highlight of particles in cross-section of cell wall of foam sample I

Fig. 12 Measurement of thickness of cell wall of foam sample I

Discussion

Application of the critical coverage ratio criterion

Based on the experimental results in Tables 3, 4, 5, the condition of foam stability keeps the same when F_V, d, or θ changes within certain range. The critical coverage ratio on the bubble interface is larger than about 14%. As these three parameters are most important parameters in gas injection foaming process, the coverage ratio on the bubble interface could be the stabilization criterion of aluminum foams in this process.

According to the stabilization criterion Eq. 5, F_V and h_c have an inversely proportional relationship when other process parameters are fixed, which has been proved in literature [8]. The experimental data in Table 3 are in agreement with this relationship.

Equation 5 shows that when other process parameters are given, the less d, the easier to satisfy the stabilization condition of the foam, proved in Table 4. It means that the smallest particles should be used for foam stability if they were able to be dispersed uniformly. h_c and d in Table 4 have not strictly positive relationship. The reason may be that the particles were not dispersed uniformly in this experiment especially for smaller particles, or different sizes of particles have different adsorption coefficients.

Equation 5 points out the influence of θ on the foam stability. Most of the researches considered the optimum wetting angle of particles to stabilize the foams is about 90° [17–20]. These phenomena can be explained by E in Eq. 5. According to the experimental data in Table 5, the critical nozzle immersion depth increases when wetting angle of Al_2O_3 decreases. That is because the wetting angle of Al_2O_3 particles θ is about 70° (Table 8) in the air injection foaming process, which is less than the ideal value 90°. And another reason is that the adsorption coefficient W decreases as θ decreases.

Table 8 Particle diameter, effective coverage ratio, and wetting angle of foam sample I

Specimen	$d_a \times 10^3$ (mm)	$d_l \times 10^3$ (mm)	$d \times 10^3$ (mm)	E	θ (°)
Foam sample I	9.51	7.84	9.98	0.908	72

Table 9 Critical coverage ratio of foam sample IV

Specimen	β_a (%)	ρ_l (mm^{-1})	$d \times 10^3$ (mm)	β_l (%)
Foam sample IV	13.53	8.74	22.75	14.13

It is unexpected that θ of Al_2O_3 particles in the gas injection foaming process is less than 90°. In general, the wetting angle between Al_2O_3 and molten aluminum is larger than 90° and the value fluctuates under different conditions [22–24]. The reason of large difference is that in the air injection foaming process, the Al_2O_3 film formed on the bubble interface would obstruct Al_2O_3 particles from protruding into the gas phase, and this action actually decreases θ of the particles according to Fig. 2. That is to say, instead of decreasing wettability of the particles, oxygen in the gas injection foaming process increases wettability of the particles.

For the batch type of gas injection foaming process, F_V and h decrease as the process proceeds. According to the criterion, there must be certain amount of melt left as residual when the process parameters no longer meet the stabilization criterion. The residual quantity could be forecast if the parameters of Eq. 5 have been determined in a given foaming process. The foam could be stabilized by increasing h when F_V is small, so changing structure of foaming mold will decrease the residual quantity.

Influence of particle agglomeration on W

According to Table 7, adsorption coefficients calculated by three methods, W_a, W_l, and W_V, are different from one another. The main reason is the particle agglomeration.

As seen in Table 6, F_V and d are larger than the particle addition value (10 vol.% and 9 μm) due to the agglomeration. It is easy to find that particle on the bubble interface is smaller than the one in the melt by comparing d in Table 6 and in Table 8. It means that smaller particles are easier to be adsorbed, which results in changing of W as process proceeds and the difference between W_a and W_l. Equation 9 is deduced from Eqs. 7 and 8, and d in Eq. 8 should be diameter of particles on the bubble interface. However, adsorption coefficients in Table 7 are calculated using diameter of particles in the melt. These two diameters are different, so the difference between W_a and W_l is great. Unfortunately, volume percentage of particles which are able to be adsorbed on the bubble interface at some

time is unknown, so only total particle volume percentage F_V could be used.

Owing to the agglomeration, adsorption coefficients calculated by Eqs. 7, 9, and 13 are average adsorption coefficient of different size of particles. Whether the average value is applicable depends on two qualifications: first, the average value can be used to calculate particle amount inside foam cell wall; second, the average value satisfies stabilization criterion Eq. 5.

W_a determined by Eq. 7 does not meet the first condition. Due to drainage in the foam cell wall, W_V calculated by Eq. 13 should be always the biggest one of the three values. Therefore, W_a is overestimated under the conditions of current particle dispersion process level.

W_V determined by Eq. 13 satisfies the first qualification apparently. However, due to drainage, particle volume percentage in foam sample will be larger than the value when the foam was just formed, particularly when particle amount or oxygen amount in gas is very small. Therefor, W_V does not satisfy the second qualification at critically stable situation.

Considering W_l calculated by Eq. 9, it is smaller than W_V, so it will satisfy the first condition by introducing correction coefficient to calculate the accurate particle volume percentage inside foam cell wall, as Eq. 21:

$$F_{Vf} = \frac{(1 - F_V \cdot R)hW_l}{2t + kF_VhW_l}F_V + F_V \cdot R, \tag{21}$$

where R denotes the correction coefficient, which is a number larger than 1.

W_l, F_{Vf}, and other foaming parameters of the four foam samples are listed in Table 10 to determine the variation law of R, where F_{Vf}' and F_{Vf}'' denotes F_{Vf} calculated by Eqs. 13 and 21, respectively. The wetting angle θ used in calculation is gotten from Table 8.

It can be seen in Table 10, the correction coefficient R increases when F_{Vf}' decreases. F_{Vf}' can be considered as the volume percentage of particles in the cell wall when the foam was just formed. The smaller the F_{Vf}', the stronger drainage in the cell wall. Thus, R should be increased to calculate the accurate F_{Vf}, and the variation law is the product of R and F_{Vf}' is about 0.21.

Discussion about W_l above mentioned shows W_l can satisfy the first condition by introducing R whose changing rule is clear.

Then, both sides of Eq. 5 were calculated using W_l and other foaming parameters of the four foam samples to

Table 10 Parameters of sample I, II, III, and IV

Specimen	F_V (%)	$d \times 10^3$ (mm)	h (mm)	ρ_1 (mm^{-1})	W_1	$t \times 10^3$ (mm)	F_{Vf}' (%)	R	F_{Vf}'' (%)	F_{Vf} (%)	$R^* F_{Vf}'$
Sample I	13.27	17.37	125	28.95	0.0011	126.7	19.53	1.05	20.14	20.15	0.21
Sample II	12.12	17.88	100	22.75	0.0013	116.3	17.87	1.21	20.25	20.25	0.22
Sample III	11.57	16.73	80	23.21	0.0015	75.5	19.54	1.10	20.60	20.60	0.21
Sample IV	4.53	22.75	60	8.74	0.0035	107.2	8.75	2.27	14.25	14.26	0.20

examine whether W_1 satisfies the second condition. The results are listed in Table 11. Most parameters are gotten from Table 10. The critical coverage ratios of four samples used in calculation are all β_a in Table 9. E is gotten from Table 8.

As seen in Table 11, calculated results using W_1 satisfy the stabilization criterion equation. Therefore, W_1 is applicable.

Generally speaking, among three methods of determining W, the workload of Eq. 13 is smallest. With the help of the changing rule of R in Table 10, W_1 can be calculated by method of measuring F_{Vf} for a smallest workload, as Eq. 22.

$$
\begin{cases}
F_{Vf} = \dfrac{(1 - F_V \cdot R)hW_1}{2t + kF_V hW_1}F_V + F_V \cdot R \\
0.21 = R \cdot \left(\dfrac{(1 - F_V)hW_1}{2t + kF_V hW_1}F_V + F_V \right)
\end{cases}, \tag{22}
$$

where R and W_1 are unknown, and W_1 can be determined by solving Eq. 22.

The variation law of R should be redetermined, when addition amount of particle is larger than 10 vol.%, or other drainage influencing conditions change, i.e., the dispersion process, the foaming temperature and the gas composition.

Particle diameter listed in Tables 3, 4, 5 is nominal value, which is different from the one measured by metallographic analysis in the second part of experiment according to discussion mentioned above. It may be the reason why critical nozzle immersion depth of melt sample IV is small although its particle size is very large compared with experimental data in Tables 3, 4, 5.

Equations 7, 9, and 13 all contain nozzle immersion depth h. Apparently, the number of particles, which can be adsorbed by a bubble, is limited. Therefore, when h is larger than a certain value, calculated value of W will

decrease as h increases. This phenomenon will be discussed in another article, with no effect on the conclusions of this article.

Simplification of determining of W_1 and β

Examine the denominator of the first term on right side of Eq. 21. It is easy to find that "$kF_V hW$" is much less than "$2t$". Therefore, Eq. 22 could be simplified to Eq. 23:

$$
\begin{cases}
F_{Vf} = \dfrac{(1 - F_V \cdot R)hW_1}{2t}F_V + F_V \cdot R \\
0.21 = R \cdot \left(\dfrac{(1 - F_V)hW_1}{2t}F_V + F_V \right)
\end{cases}. \tag{23}
$$

As seen in Table 9, the critical coverage ratio calculated by Eq. 20, β_1, is almost equal to the directly measured value β_a. That shows the indirect measuring method is reasonable. According to Eqs. 9 and 14, Eq. 20 could be written as:

$$
\beta_1 = \frac{3hF_V E}{8d}W_1. \tag{24}
$$

Therefore, β could be determined by combining Eqs. 23 and 24, when the foam is critically stable. The measurement is done on the cross-section of the foam cell wall with smaller workload.

β is strongly influenced by gas composition [8, 10], and has relation with the foaming temperature [16]. Specifically, when oxygen amount in the foaming gas decreases, β increases. However, when the foaming temperature decreases, β decreases. Therefore, when these parameters change, β needs to be redetermined.

Conclusion

(1) The coverage ratio on the bubble interface is the stabilization criterion of aluminum foam in the gas injection foaming process. At given gas composition and foaming temperature, the necessary condition of foam stability is always that the coverage ratio on the bubble interface should be larger than a critical value.

(2) The product of the ceramic particle volume percentage and the nozzle immersion depth should be larger

Table 11 Examination of stabilization criterion of foam samples

Specimen	hF_V (mm)	$8d\beta_a/3W_1E$ (mm)
Foam sample I	16.59	8.52
Foam sample II	12.12	7.48
Foam sample III	9.26	6.39
Foam sample IV	2.72	2.63

than a certain value when the gas composition and the foaming temperature are fixed. This value is determined by particle size, critical coverage ratio, adsorption coefficient, and particle wettability.

(3) The adsorption coefficient of particles could be determined by several methods. Due to difficulty of the dispersion process, the method of measuring particle area density on the bubble interface has big fluctuation. The value determined by measuring particle linear density on the bubble interface by observing the cross-section of the cell wall is applicable. As the adsorption coefficients of different size of particles are different, the average adsorption coefficient changes as foaming process proceeds.

(4) The method of measuring particle amount inside foam cell wall to determine the adsorption coefficient has smallest workload. Though at some situations the drainage will give rise to error, it can be eliminated by introducing a correction coefficient.

(5) The wetting angle of Al_2O_3 particles in the gas injection foaming process under this experimental condition (air injection into A356 melt, foaming at 700 °C) is about 70°, and the effective coverage ratio of Al_2O_3 particle is about 0.9.

(6) The critical coverage ratio on the bubble interface under this experimental condition is about 14%. Except for direct measuring on the surface of cell wall, the critical coverage ratio can be indirectly calculated using the average adsorption coefficient.

Appendix

Relationship between two-dimensional diameter measured by metallographic analysis and real diameter of the particle

When measuring the diameter of particles in matrix by metallographic analysis, different sections of the particle will be observed, like d_1, d_2 and so on (Fig. 13). If the image analysis software calculates the diameter of every section firstly and their average secondly, then the measured two-dimensional diameter d'_1 is as Eq. 25. If the software calculates the area of every section firstly, their average secondly, and the equivalent diameter of the average area finally, then the two-dimensional diameter d'_2 is as Eq. 26. Distribution of these sections is random. When there are lots of sections, Eqs. 27 and 28 could be got by calculus. Therefore, the two-dimensional diameter has two forms as Eqs. 29 and 30. In this article, the image
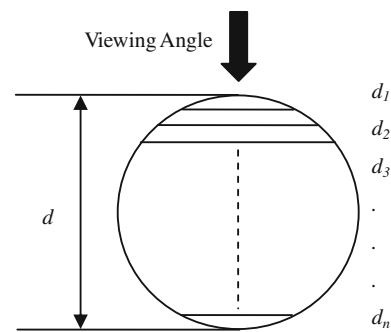

Fig. 13 Particle observation by metallographic analysis

analysis software uses the first measurement principle, so d and d' have a relationship like Eq. 29.

When observing cross-section of the foam cell wall, different sections of the particle on the bubble interface could be seen, like Fig. 13. Therefore, the real diameter of particles on the bubble interface can be calculated by d_1 as Eq. 15. When observing surface, because of particle wettability, only certain section could be seen. Therefore, the particle wetting angle can be calculated by d_1 and d_a as Eq. 16:

$$d'_1 = \frac{d_1 + d_2 + \cdots + d_n}{n}, \tag{25}$$

$$d'_2 = \sqrt{\frac{d_1^2 + d_2^2 + \cdots + d_n^2}{n}}, \tag{26}$$

$$(d_1 + d_2 + \cdots + d_n)\frac{d}{n} = \frac{\pi}{4}d^2, \tag{27}$$

$$\frac{\pi}{4}(d_1^2 + d_2^2 + \cdots + d_n^2)\frac{d}{n} = \frac{\pi}{6}d^3, \tag{28}$$

$$d'_1 = \frac{\pi}{4}d, \tag{29}$$

$$d'_2 = \frac{\sqrt{6}}{3}d. \tag{30}$$

References

1. Stobener K, Rausch G (2009) J Mater Sci 44(6):1506. doi: 10.1007/s10853-008-2786-8
2. Cluff DRA, Esmaeili S (2009) J Mater Sci 44(14):3867. doi: 10.1007/s10853-009-3525-5
3. Bonaccorsi L, Proverbio E, Raffaele N (2010) J Mater Sci 45(6):1514. doi:10.1007/s10853-009-4115-2
4. Chen X, Li YX (2003) Mater Rev 17(5):5
5. Banhart J (2001) Prog Mater Sci 46:559
6. Lefebvre L-P, Banhart J, Dunand DC (2008) Advanced Engineering Materials 10(9):775
7. Jin I, Kenny LD, Sang H (1990) US Patent 4973358
8. Leitlmeier D, Degischer HP, Flankl HJ (2002) Adv Eng Mater 4(10):735

9. Karsu ND, Yuksel S, Guden M (2009) J Mater Sci 44(6):1494. doi:10.1007/s10853-008-3039-6
10. Babcsán N, Leitlmeier D, Degischer HP, Banhart J (2004) Adv Eng Mater 6(6):421
11. Babcsán N, Garcia-Moreno F, Banhart J (2006) Role of oxidation during blowing of aluminium foams by external gas injection. Porous metals, metal foaming technology (MetFoam 2005). The Japan Institute of Metals, Japan, p 261
12. Banhart J (2006) Adv Eng Mater 8(9):781
13. Babcsán N, Leitlmeier D, Degischer HP (2003) Materialwissenschaft und werkstofftechnik (Mater Sci Eng Technol) 34(1):22
14. Gergely V, Jones L, Clyne TW (2001) Trans JWRI 30(Special Issue):371
15. Kaptay G (2004) Colloids Surf A 230(1–3):67
16. Ip SW, Wang Y, Toguri JM (1999) Can Metall Q 38:81–92
17. Babcsán N, Leitlmeier D, Banhart J (2005) Colloids Surf A 261(1–3):123
18. Sun YQ, Gao T (2002) Metall Mater Trans A 33(10):3285
19. Kaptay G (2006) Colloids Surf A 282–283:387
20. Klinter AJ, Leon CA, Drew RAL (2010) J Mater Sci 45(8):2174. doi:10.1007/s10853-009-4056-9
21. Laurent V, Rado C, Eustathopoulos N (1996) Mater Sci Eng A 205(1–2):1
22. Shen P, Fujii H, Matsumoto T, Nogi K (2003) Scr Mater 48(6):779
23. Shen P, Fujii H, Nogi K (2006) J Mater Sci 41(21):7159. doi:10.1007/s10853-006-0924-8
24. Chang H, Higginson R, Binner J (2010) J Mater Sci 45(3):662. doi:10.1007/s10853-009-3983-9